

# ISOTHERMAL AMORPHOUS-AMORPHOUS-AMORPHOUS TRANSITIONS IN WATER

K. Winkel<sup>1</sup>, W. Schustereder<sup>1,2</sup>, I. Kohl<sup>1</sup>, C. G. Salzmann<sup>1,4</sup>, E. Mayer<sup>1</sup>, T. Loerting<sup>1,3</sup>

<sup>1</sup> Institute of General, Inorganic and Theoretical Chemistry, University of Innsbruck, Innrain 52a, A-6020 Innsbruck, Austria

<sup>2</sup> Max-Planck-Institute for Plasma-Physics, EURATOM Association, Boltzmannstr. 2, D-85748 Garching, Germany

<sup>3</sup> Institute of Physical Chemistry, University of Innsbruck, Innrain 52a, A-6020 Innsbruck

<sup>4</sup> Inorganic Chemistry Lab, University of Oxford, South Parks Road, OX1 3QR United Kingdom

## 1 INTRODUCTION

Polyamorphism is a fundamental phenomenon, which is believed to be linked to the occurrence of two or even more liquids in one-component systems<sup>1</sup>. It is furthermore thought that a possible occurrence of multiple liquids in one-component systems is intimately linked with their anomalous properties, such as negative thermal expansion coefficients or isothermal compressibility maxima<sup>2,4</sup>. Polyamorphism has been observed since its discovery on the example of water<sup>5</sup> in many one-component substances<sup>6-8</sup>. Probably the most extensively investigated “anomalous” liquid is water, which shows “typical” behaviour at high temperatures, whereas its anomalies become stronger on cooling into its supercooled state<sup>9-12</sup>. For instance the thermal expansion coefficient is positive at  $T > 277$  K, but negative at  $T < 277$  K. The anomalies disappear not only on heating, but also on increasing the pressure to  $P > 200$  MPa, where e.g. the dynamic viscosity and the self diffusion coefficient show the typical pressure dependence found for most of the liquids, e.g., organic liquids, van-der-Waals liquids or metal melts. To explain these anomalies “water’s second critical point” has been postulated<sup>13</sup>. There are supposedly two liquid states, which can not be discerned at the “second critical point”, which are called “low density liquid” (LDL) and “high density liquid” (HDL) and which are separated by a first-order phase transition. This second critical point is postulated to be at a pressure  $p \sim 17 - 340$  MPa and at a temperature  $T \sim 145 - 230$  K<sup>14-18</sup>. Unfortunately, this  $p$ - $T$  area is not accessible for direct experiments with liquid water, since most of it is located in the “no man’s land”, where only crystalline ice is observed.

Therefore, experiments are performed on “immobilized liquids”, or in other words on amorphous water (also called vitreous water or glassy water)<sup>19</sup>. Currently, three structurally distinct amorphous states of water are known: low- (LDA)<sup>5,20</sup>, high- (HDA)<sup>20,21</sup> and very high- (VHDA) density amorphous ice<sup>22,23</sup>. We emphasize that HDA is not a well defined state but rather comprises a number of substates. It has been suggested to use the nomenclature “uHDA” (“unrelaxed HDA”)<sup>24</sup>, “eHDA” (“expanded HDA”)<sup>24</sup> and/or “rHDA” (“relaxed HDA”)<sup>25,26</sup> to account for this. Even though no signs of microcrystallinity have been found in neutron or X-ray diffraction studies, it is unclear whether

HDA and VHDA are truly immobilized liquids, i.e., if they are truly related to a high-density liquid (HDL) and very-high density liquid (VHDL). It has been argued that HDA is in fact a mechanically collapsed crystal unrelated to HDL<sup>27</sup>. Whereas there seems to be a discontinuity in density upon transforming LDA to HDA<sup>5</sup>, which supports the liquid-liquid transition hypothesis, the experimental data is ambiguous whether there is also a discontinuity in density upon transforming HDA to VHDA<sup>28</sup>. Hence, it is unclear if there might even be a third or fourth critical point in water's phase diagram related to a liquid-liquid transition in a one component system as proposed in some computer simulations<sup>29-33</sup>, whereas others show only two critical points<sup>34-37</sup>. Some hints for multiple liquid-liquid transitions have been provided from an infrared spectroscopy study<sup>38</sup>, but clear experimental evidence is missing.

Herein, we expand on the discussion of our recently observed isothermal amorphous-amorphous transition sequence<sup>23</sup>. We achieved to compress LDA in an isothermal, dilatometric experiment at 125 K in a stepwise fashion *via* HDA to VHDA. However, we can not distinguish if this stepwise process is a kinetically controlled continuous process or if both steps are true phase transitions (of first or higher order). We want to emphasize that the main focus here is to investigate transitions between different amorphous states *at elevated pressures* rather than the annealing effects observed *at 1 bar*. The vast majority of computational studies shows qualitatively similar features in the metastable phase diagram of amorphous water (cf. e.g. Fig.1 in ref. 39): at elevated pressures the *thermodynamic equilibrium line* between HDA and LDA can be reversibly crossed, whereas by heating at 1 bar the *spinodal* is irreversibly crossed. These two fundamentally different mechanisms need to be scrutinized separately.

## 2 METHODS

In brief, 300 mg of LDA are prepared in a piston-cylinder apparatus with a bore diameter of 8 mm by compressing ice Ih to HDA at 77 K to 1.5 GPa and by subsequent heating of HDA at 0.020 GPa. This protocol was shown to reliably produce LDA with the maximum of the first diffraction peak at  $2\theta=24^\circ$  ( $d=0.37$  nm)<sup>40</sup>. After quenching to 77 K and recovery to 1 bar samples are characterized using powder X-ray diffraction. All diffractograms were recorded at 83 – 88 K in  $\theta$ - $2\theta$  geometry employing Cu-K $\alpha$  rays ( $\lambda=0.154$  nm) using a Siemens D-5000 diffractometer equipped with a low-temperature camera from Anton Paar. The sample plate was in horizontal position during the whole measurement. Installation of a "Goebel mirror" allowed us to use small amounts of sample without distortion of the Bragg peaks. Neither any crystalline by-products nor any remnants of HDA can be detected using powder X-ray diffraction. LDA is encased in a container of indium, which is a ductile metal also at 77 K, and which prevents shock-wave heating of the ice on compression to pressures up to 2 GPa<sup>41</sup>. LDA is then compressed isothermally at 20 MPa/min at 77 K, 100 K or 125 K, quenched to 77 K at elevated pressures and finally decompressed to ambient pressure at -20 MPa/min. Typically, the temperature varies by  $\pm 1$  K at 125 K at 100 K, and up to  $\pm 2$  K during the transition events, whereas it is essentially constant for experiments performed at 77 K.

## 3 RESULTS

In Fig. 1a the raw data for three compression/decompression experiments up to 1.5 GPa starting with LDA at 125 K are shown. The piston displacement measured after pre-

compression to 0.1 GPa serves as the origin (piston displacement = 0). Despite of the slight temperature oscillations up to  $\pm 2$  K the reproducibility is excellent - all three curves are almost identical. There is a sharp step in piston displacement of about 1.1 mm in the range 0.4 – 0.5 GPa and a broader step of about 0.6 mm in the range 0.8 – 1.0 GPa. After decompression an overall densification of 1.6 mm is observed in all three cases. The midpoint of the transformation for the first density step attributed to the LDA→HDA transformation varies in the pressure range 0.44 – 0.48 GPa for the three experiments shown in Fig.1a and additional eight experiments done in the same manner with the exception that quenching and decompression was initiated at 0.7 GPa (not shown). This variation is possibly related to small differences in temperature or to other effects beyond our control. The statistical variation of nominal pressures of transformation from LDA to HDA at 125 K is hence  $\pm 0.02$  GPa. The piston displacement at a pressure of 0.6 GPa varies by no more than  $\pm 0.15$  mm for eleven experiments, which implies a variation of about 14% in the step height.

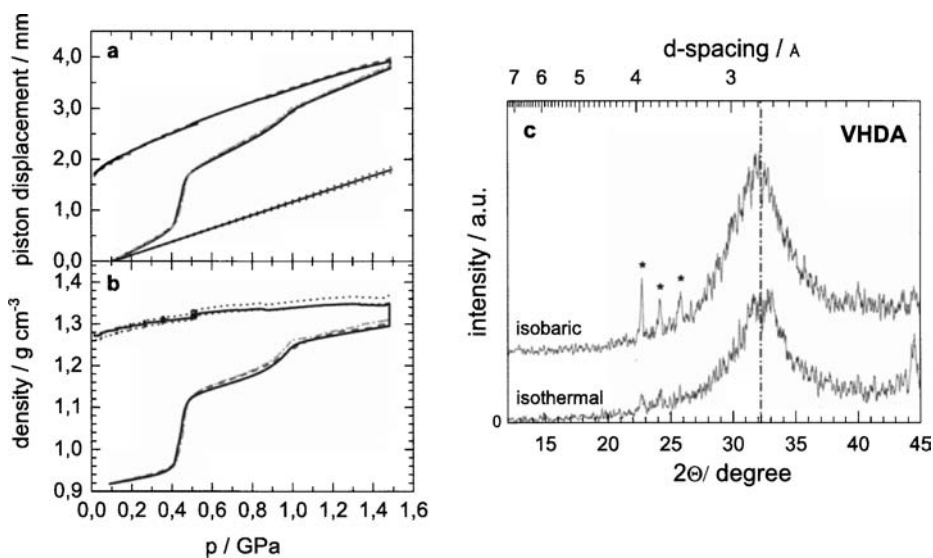


**Figure 1** (a) Three curves of “raw” piston displacement data obtained on compressing LDA at 125 K (top curves) together with the apparatus correction  $d^0(p)$  (straight line at bottom). (b) “Processed” density data (see text) (c) Powder X-ray diffractograms of the final recovered states (bottom) in comparison with the powder X-ray diffractogram of VHDA obtained by annealing HDA at 1.1 GPa<sup>22</sup> (top). The dashed line is intended to guide the eye to the location of the maximum of the first broad diffraction peak. Stars indicate positions of reflexes caused by traces of Ih, which had formed by condensation of water vapour during transfer of sample onto the precooled X-ray sample holder (cf. ref. 42). The sample itself is fully amorphous.

The X-ray diffractogram obtained from the recovered state after one of these experiments is shown in Fig. 1c (bottom). This X-ray diffractogram is directly compared to an X-ray diffractogram obtained from a recovered sample of VHDA as prepared by annealing HDA to  $\sim 160$  K at 1.1 GPa (top)<sup>22</sup>. Both diffractograms are very similar, with a first broad

diffraction maximum at  $2\theta=32.3\pm 0.2^\circ$  and can both be defined as VHDA (in accordance with the definition that all HDA states annealed under pressures above 0.8 GPa should be called VHDA)<sup>26</sup>.

In order to calculate *in situ* densities from the piston displacement data a reference density is required, which is in our case the density  $\rho(\text{LDA})=0.92\pm 0.02 \text{ g/cm}^3$  at 125 K<sup>43</sup>. Furthermore, it is necessary to subtract the piston displacement obtained in a blind experiment, i.e., the same experiment, but without ice (bottom curve in Fig. 1a). This blind experiment was previously called “indium correction”<sup>20,28</sup>. However, the correction functions  $d^0(p)$  recorded with 350 mg of indium and no ice (solid line) and the correction functions recorded with no indium and no ice (dashed line) shown in Fig. 2c indicate that the correction function is dominated by the compressibility of the piston-cylinder apparatus and the frame of the material testing machine, whereas the indium contribution is negligible. The *in situ* density  $\rho(p)$  can be calculated using the mass of ice  $m(\text{ice } I_h)$  and the cross-section of the bore  $A$  from the difference in piston displacement  $\Delta d(p)$  (“real experiment”  $d(p)$  minus “blind experiment”  $d^0(p)$ ) as

$$\rho(p) = \rho(\text{LDA}) \times (A^{-1} \times m(\text{ice } I_h) \times \rho(\text{ice } I_h)^{-1} - \Delta d(p))^{-1} \times A^{-1} \times m(\text{ice } I_h) \times \rho(\text{ice } I_h)^{-1} \quad (1)$$

The results of this correction procedure are shown in Fig. 1b. The density steps can be quantified to be  $\sim 20\%$  at 0.45 GPa and  $\sim 5\%$  at 0.95 GPa. The second density step decreases to  $\sim 1\%$  upon employing higher compression rates of 600 or 6000 MPa/min, whereas the first density step remains essentially unchanged. This might imply that the activation barrier from LDA to HDA is lower than the activation barrier from HDA to VHDA<sup>23</sup>. From the data shown in Fig. 1b, the isothermal compressibility  $\kappa_T$  can easily be calculated by differentiation (cf. Fig. 3, bottom panel in ref. 23). It shows two maxima and reaches at least five times the isothermal compressibilities  $\kappa_T$  of LDA and HDA in the course of the transformation.

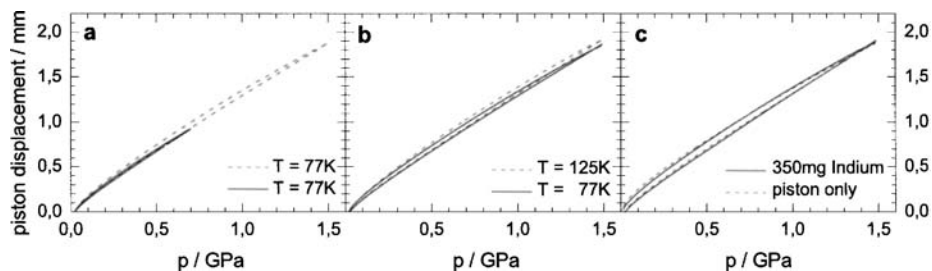


**Figure 2** Correction function  $d^0(p)$  obtained using different experimental parameters. (a) Piston-cylinder apparatus lined with 300 mg of indium upon compression to 1.5 GPa at 77 K (dashed line) as compared to compression to 0.7 GPa (solid line). The hysteresis upon decompression is evident. (b) Effect of temperature increase from 77 K (solid line) to 125 K (dashed line). (c) Comparison of compression/decompression curves for piston-cylinder apparatus lined with 300 mg of indium (solid line) and without indium (dashed line). The effect of different compression rates ranging from 6 MPa/min to 6 GPa/min was found to be negligible.

Figs. 2a-c show various blind experiments  $d^0(p)$  obtained in a compression/decompression cycle. Fig.2a compares a blind experiment conducted on compressing up to 0.7 GPa (solid line) and up to 1.5 GPa (dashed line), all other parameters being equal. It is evident that there is a hysteresis of up to 0.1 mm at intermediate pressures and also a slight hysteresis after full decompression. The hysteresis is much more pronounced for the experiment conducted up to 1.5 GPa. It is, therefore, necessary to use two separate correction functions  $d^0(p)$  for the compression part and the decompression part, especially for experiments conducted in the range 0-1.5 GPa, or even higher. It is not valid to extrapolate correction functions  $d^0(p)$  to higher pressures.

For our previous calculation of the density of VHDA after recovery to 77 K and 1 bar (cf. Fig. 1 in ref. 23) we have assumed a constant bore diameter of 8.0 mm, and have arrived at an unreasonably high value of  $\sim 1.31 \text{ g/cm}^3$ , rather than the accepted VHDA density of  $1.25 \pm 0.01 \text{ g/cm}^3$  measured by two independent methods, namely flotation of VHDA in a liquid  $\text{N}_2/\text{Ar}$  mixture and isobaric expansion of VHDA to LDA by heating at 1 bar and quenching to 77 K<sup>22</sup>. Furthermore, we saw spurious effects, such as a slight increase of density on decompressing from 1.5 GPa to 1.0 GPa. For the graph shown in Fig. 1b we use a bore diameter of 7.8 mm, since we want to take into account the fact that a  $\sim 100 \text{ }\mu\text{m}$  thick indium foil is wrapped around the sample. We do not take into account the contraction of the bore diameter upon cooling from ambient conditions to 77 K, since we do not know the thermal expansivity of our steel cylinder. Using 7.8 mm for the bore diameter, a density of  $1.27 \text{ g/cm}^3$  results for VHDA, which is close to the accepted value, and the spurious density increase upon decompression disappears at well. Using a diameter less than 7.8 mm we arrive at a density of  $1.25 \text{ g/cm}^3$ . We, therefore, conclude that the exact diameter available to the sample is important in quantifying its density. Since we do not know it exactly the density given in Fig. 1b is accurate only to  $\pm 0.02 \text{ g/cm}^3$ . In addition to the error by the unknown bore diameter, the error in the density of LDA of  $\pm 0.02 \text{ g/cm}^3$  also contributes to the total error<sup>43</sup>.

We want to point out that the densities reported in Fig.1b are lower than the densities reported by some of us in a different study<sup>26</sup>. For instance at 1.0 GPa the density in Fig. 1b reads as  $1.26 \text{ g/cm}^3$ , whereas it reads as  $1.33 \text{ g/cm}^3$  in Fig.2 of ref. 26. We believe that the latter densities are the correct ones to believe a) because highly accurate densities of crystalline material *at elevated pressures* were used as a reference for the calculation (whereas for the data in Fig.1b the density  $\rho(\text{LDA})=0.92 \pm 0.02 \text{ g/cm}^3$  at 1bar serves as the reference) and b) because these data refer to crystallization temperature, e.g.,  $\sim 165 \text{ K}$  at 1.0 GPa rather than to 125 K. An increase in temperature at elevated pressures was recently shown to cause significant structural relaxation effects in HDA<sup>24</sup>. Whereas at a pressure of  $\sim 0.2 \text{ GPa}$  this causes the formation of “expanded HDA” of lower density<sup>24</sup>, it is very likely that at much higher pressures such as 1.0 GPa similar relaxation effects cause the formation of “compressed HDA” of higher density. That is, on increasing the temperature from 125 K to 165 K at 1.0 GPa structural relaxation may increase the density from  $1.26 \text{ g/cm}^3$  to  $1.33 \text{ g/cm}^3$ . For the reason of this missing equilibration at 125 K we are not able to say if the second density step is related solely to a kinetic process or a combined thermodynamic and kinetic process.

Fig.2b shows that the temperature effect is much smaller than the hysteresis effect shown in Fig. 2a, at least in the range from 77 K to 125 K. The difference amounts to less than 0.1 mm at a pressure of 1.5 GPa and much less than 0.1 mm at a pressure of 0.7 GPa. For comparison quenching of VHDA from 125 K to 77 K at 1.5 GPa causes a change of  $\sim 0.20 \text{ mm}$  (cf. Fig. 1a) and quenching of HDA from 125 K to 77 K at 0.7 GPa causes a change of  $\sim 0.17 \text{ mm}$  (cf. Fig. 3a). That is, the thermal expansion of HDA and VHDA exceeds the thermal expansion of the apparatus and indium. Nevertheless, the temperature

effect on the apparatus correction is not negligible. As already mentioned above, Fig.2c shows that, at least for compression experiments, indium does not contribute significantly to the correction function. Please note, that this might be different for isobaric heating/cooling experiments.

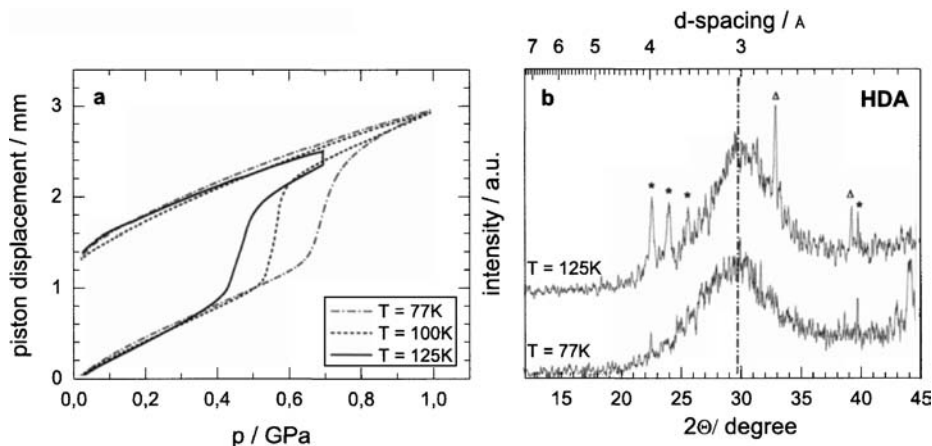


**Figure 3** (a) “Raw” piston displacement data for the 1<sup>st</sup> density step obtained on compression of LDA at 77 K (dashed line), 100 K (dotted line) and 125 K (solid line). The final density after recovery calculates as  $1.15 \pm 0.01 \text{ g/cm}^3$  in all three cases. (b) Powder X-ray diffractograms of the recovered samples compressed at 125 K (top) and 77 K (bottom). For details cf. the caption to Fig. 1c. Triangles indicate peaks arising from indium contamination.

In Fig. 3a we show three pressure vs. piston displacement curves obtained on compression of LDA and related to the first density step. The main difference is the compression temperature. Whereas the second density step is not observable at 77 K at pressures up to 1.6 GPa<sup>5</sup>, the first density step is observable also at these temperatures. This might again imply that the activation barrier from LDA to HDA is lower than the activation barrier from HDA to VHDA. As also observed by Mishima<sup>44</sup> the pressure required to transform LDA to HDA decreases as the temperature increases, namely from  $\sim 0.70 \text{ GPa}$  at 77 K to  $\sim 0.55 \text{ GPa}$  at 100 K and to  $\sim 0.45 \text{ GPa}$  at 125 K. The height of the step remains the same. All decompression curves of HDA reach a final piston displacement of  $\sim 1.4 \text{ mm}$ , which implies that the densities of all three samples are roughly equal after recovery. It amounts to  $1.15 \pm 0.01 \text{ g/cm}^3$  after the correction procedure described above. Please note that the dashed curve at 100 K was recorded without quenching to 77 K, i.e., a conversion back to LDA does not take place also at 100 K. In Fig. 3b we show the X-ray diffractograms of the samples compressed at 77 K (bottom) and 125 K (top). On ignoring the sharp features arising from tiny amounts of condensed hexagonal ice and indium both diffractograms are very similar with a first broad maximum at  $2\theta \sim 30.5 \pm 0.3^\circ$ . However, both are clearly different from the diffractograms shown in Fig. 1c and show the maximum at about the position expected for HDA<sup>20,45-49</sup>. We want to emphasize that the diffractogram shown here (Fig.3b, top) is different from the one shown as diffractogram B before by us<sup>23,28</sup> in the sense that the first broad diffraction maximum is shifted by about  $2\theta \sim 1^\circ$ . Also heterogeneity as indicated by small angle scattering<sup>50</sup> is no longer evident. The diffractogram to rely on is the one shown in Fig.3b rather than the earlier one, which probably suffered from slight annealing at 1 bar during sample transfer, which is known to

be at the origin of such a shift in the diffraction maximum<sup>20,51,52</sup> and to induce heterogeneity<sup>50</sup>. The X-ray diffractograms of HDA can not be obtained by co-adding X-ray diffractograms of LDA and VHDA in different ratios. This typically produces diffractograms showing a broad double maximum and a minimum in between located at  $2\theta\text{--}30^\circ$  ( $d\text{--}0.30$  nm). According to this X-ray diffraction evidence, HDA produced upon isothermal compression of LDA is, therefore, not a mixture of LDA and VHDA up to the length scales probed with our equipment, i.e.,  $\sim 7$  Å. On the other hand neutron diffraction shows that all the amorphous states obtained in the course of the HDA→LDA transition at  $\sim 0.3$  GPa and 130 K can be expressed as a linear combination of LDA and HDA<sup>53</sup>. This supports the picture of a first order phase transition between LDA and HDA at 130 K, whereas the transition between LDA and VHDA at 125 K is clearly not a single first-order phase transition, but rather a combined process.

#### 4 CONCLUSIONS

We conclude that we have observed an amorphous-amorphous-amorphous transition from LDA to VHDA *via* HDA. We can not distinguish if these are phase transitions in the sense of a first or higher order transition or if these are continuous annealing processes governed by accelerating/decelerating kinetics. In the case of  $\alpha\text{-SiO}_2$ , the only other case for which such an amorphous-amorphous-amorphous transition has been observed, the authors infer that it is not a first-order transition<sup>54</sup>. Furthermore, we discuss how the raw pressure vs. piston displacement data is converted to pressure vs. sample density data by subtracting the blind experiment without ice, which was previously called “indium correction”. We show that the indium itself, used as a lubricant at 77 K, contributes negligibly to the “apparatus correction”. We furthermore point out that calculation of accurate absolute  $\rho(p)$  curves requires knowledge of the diameter available to the sample, as well as an “apparatus correction” recorded at exactly the same conditions both for the compression as well as for the decompression step (hysteresis and temperature effects!), which we did not properly account for previously<sup>23</sup>. This explains why we (erroneously) calculated a density of  $1.31$  g/cm<sup>3</sup> for VHDA at 77 K and 1 bar in Fig. 1 of ref. 23. On doing the correction procedure properly we obtain a value of  $1.27\pm 0.02$  g/cm<sup>3</sup> from the density data, which is close to the accepted value of  $1.25\pm 0.01$  g/cm<sup>3</sup>.

#### Acknowledgements

We are thankful to Prof. Erminald Bertel for discussions and grateful to the Austrian Science Fund FWF (project no R37-N11) for financial support. I.K. acknowledges support by the Austrian Academy of Sciences (APART-programme).

#### References

- 1 P. G. Debenedetti, *Nature*, **392**, 127 (1998).
- 2 C. A. Angell, R. D. Bressel, M. Hemmati, et al., *PCCP*, **2**, 1559 (2000).
- 3 H. Tanaka, *Europhys. Lett.*, **50**, 340 (2000).
- 4 V. V. Brazhkin and A. G. Lyapin, *J. Phys.: Cond. Matter*, **15**, 6059 (2003).
- 5 O. Mishima, L. D. Calvert, and E. Whalley, *Nature*, **314**, 76 (1985).
- 6 S. M. Sharma and S. K. Sikka, *Prog. Mater. Sci.*, **40**, 1 (1996).
- 7 P. H. Poole, T. Grande, C. A. Angell, et al., *Science*, **275**, 322 (1997).
- 8 P. F. McMillan, *J. Mater. Chem.*, **14**, 1506 (2004).

- 9 C. A. Angell, in *Water Compr. Treatise* (1982), Vol. 7, p. 1.
- 10 P. G. Debenedetti, *J. Phys.: Cond. Matter*, **15**, R1669 (2003).
- 11 P. G. Debenedetti and H. E. Stanley, *Physics Today*, **56**, 40 (2003).
- 12 C. A. Angell, *Annu. Rev. Phys. Chem.*, **55**, 555 (2004).
- 13 P. H. Poole, F. Sciortino, U. Essmann, et al., *Nature*, **360**, 324 (1992).
- 14 E. G. Ponyatovsky, V. V. Sinitsyn, T. A. Pozdnyakova, *JCP*, **109**, 2413 (1998).
- 15 H. E. Stanley, M. C. Barbosa, S. Mossa, et al., *Physica A*, **315**, 281 (2002).
- 16 S. B. Kiselev and J. F. Ely, *J. Chem. Phys.*, **116**, 5657 (2002).
- 17 R. C. Dougherty, *Chem. Phys.*, **298**, 307 (2004).
- 18 H. Kanno and K. Miyata, *Chem. Phys. Lett.*, **422**, 507 (2006).
- 19 P. G. Debenedetti and F. H. Stillinger, *Nature*, **410**, 259 (2001).
- 20 O. Mishima, L. D. Calvert, and E. Whalley, *Nature*, **310**, 393 (1984).
- 21 T. Loerting, I. Kohl, W. Schustereder, et al., *Chem. Phys. Chem.*, **7**, 1203 (2006).
- 22 T. Loerting, C. Salzmann, I. Kohl, et al., *PCCP*, **3**, 5355 (2001).
- 23 T. Loerting, W. Schustereder, K. Winkel, et al., *Phys. Rev. Lett.*, **96**, 025702 (2006).
- 24 R. J. Nelmes, J. S. Loveday, T. Straessle, et al., *Nature Physics*, **2**, 414 (2006).
- 25 M. Guthrie, J. Urquidi, C. A. Tulk, et al., *Phys. Rev. B*, **68**, 184110 (2003).
- 26 C. G. Salzmann, T. Loerting, S. Klotz, et al., *PCCP*, **8**, 386 (2006).
- 27 J. S. Tse, *J. Chem. Phys.*, **96**, 5482 (1992).
- 28 T. Loerting, K. Winkel, C. G. Salzmann, et al., *PCCP*, **8**, 2810 (2006).
- 29 I. Brovchenko, A. Geiger, and A. Oleinikova, *J. Chem. Phys.*, **118**, 9473 (2003).
- 30 S. V. Buldyrev and H. E. Stanley, *Physica A*, **330**, 124 (2003).
- 31 I. Brovchenko, A. Geiger, and A. Oleinikova, *J. Chem. Phys.*, **123**, 044515 (2005).
- 32 P. Jedlovsky and R. Vallauri, *J. Chem. Phys.*, **122**, 081101 (2005).
- 33 I. Brovchenko and A. Oleinikova, *J. Chem. Phys.*, **124**, 164505 (2006).
- 34 N. Giovambattista, H. E. Stanley, and F. Sciortino, *Phys. Rev. E*, **72**, 031510 (2005).
- 35 N. Giovambattista, H. E. Stanley, and F. Sciortino, *Phys. Rev. Lett.*, **94**, 107803 (2005).
- 36 R. Martonak, D. Donadio, and M. Parrinello, *Phys. Rev. Lett.*, **92**, 225702 (2004).
- 37 R. Martonak, D. Donadio, and M. Parrinello, *J. Chem. Phys.*, **122**, 134501 (2005).
- 38 D. E. Khostariya, A. Zahl, T. D. Dolidze, et al., *Chem. Phys. Chem.*, **5**, 1398 (2004).
- 39 E. G. Ponyatovsky, *J. Phys.: Cond. Matter*, **15**, 6123 (2003).
- 40 C. G. Salzmann, I. Kohl, T. Loerting, et al., *PCCP*, **5**, 3507 (2003).
- 41 I. Kohl, E. Mayer, and A. Hallbrucker, *PCCP*, **3**, 602 (2001).
- 42 C. G. Salzmann, E. Mayer, and A. Hallbrucker, *PCCP*, **6**, 5156 (2004).
- 43 V. F. Petrenko and R. W. Whitworth, *Physics of Ice* (Oxford University Press, 1999).
- 44 O. Mishima, *J. Chem. Phys.*, **100**, 5910 (1994).
- 45 L. Bosio, G. P. Johari, and J. Teixeira, *Phys. Rev. Lett.*, **56**, 460 (1986).
- 46 A. Bizid, L. Bosio, A. Defrain, et al., *J. Chem. Phys.*, **87**, 2225 (1987).
- 47 H. Schober, M. M. Koza, A. Tolle, et al., *Phys. Rev. Lett.*, **85**, 4100 (2000).
- 48 M. Guthrie, C. A. Tulk, C. J. Benmore, et al., *Chem. Phys. Lett.*, **397**, 335 (2004).
- 49 J. S. Tse, D. D. Klug, M. Guthrie, et al., *Phys. Rev. B*, **71**, 214107 (2005).
- 50 H. Schober, M. Koza, A. Tölle, et al., *Physica B*, **241-243**, 897 (1998).
- 51 C. A. Tulk, C. J. Benmore, J. Urquidi, et al., *Science*, **297**, 1320 (2002).
- 52 M. M. Koza, H. Schober, H. E. Fischer, et al., *J. Phys. Cond. Matt.*, **15**, 321 (2003).
- 53 S. Klotz, T. Straessle, R. J. Nelmes, et al., *Phys. Rev. Lett.*, **94**, 025506 (2005).
- 54 A. G. Lyapin, V. V. Brazhkin, E. L. Gromnitskaya, et al., *NATO Science Series, II: Mathematics, Physics and Chemistry*, **81**, 449 (2002).